

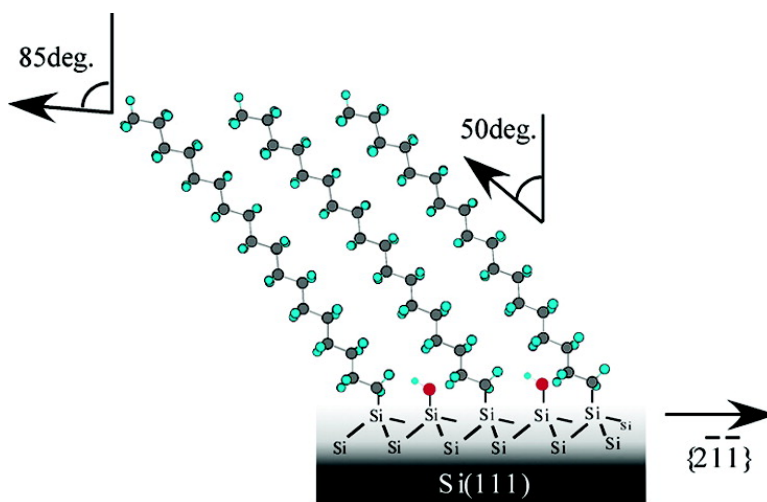
Article

Evidence for Epitaxial Arrangement and High Conformational Order of an Organic Monolayer on Si(111) by Sum Frequency Generation Spectroscopy

Satoshi Nihonyanagi, Dai Miyamoto, Satoru Idojiri, and Kohei Uosaki

J. Am. Chem. Soc., **2004**, 126 (22), 7034-7040 • DOI: 10.1021/ja049911p • Publication Date (Web): 15 May 2004

Downloaded from <http://pubs.acs.org> on March 31, 2009



More About This Article

Additional resources and features associated with this article are available within the HTML version:

- Supporting Information
- Links to the 6 articles that cite this article, as of the time of this article download
- Access to high resolution figures
- Links to articles and content related to this article
- Copyright permission to reproduce figures and/or text from this article

[View the Full Text HTML](#)

Evidence for Epitaxial Arrangement and High Conformational Order of an Organic Monolayer on Si(111) by Sum Frequency Generation Spectroscopy

Satoshi Nihonyanagi, Dai Miyamoto, Satoru Idojiri, and Kohei Uosaki*

Contribution from the Division of Chemistry, Graduate School of Science,
Hokkaido University, Sapporo 060-0810, Japan

Received January 6, 2004; E-mail: uosaki@pcl.sci.hokudai.ac.jp

Abstract: The structure of an octadecyl monolayer formed on a hydrogen-terminated Si(111) surface in neat octadecene was studied by infrared-visible sum frequency generation (SFG) spectroscopy. The SFG spectra in the CH vibration region were dominated by peaks corresponding to those of the methyl group, confirming that the monolayer is essentially in the all-trans conformation. The shapes of the spectra were strongly dependent on the azimuthal angle, and the strength of the asymmetric vibration mode obtained from the theoretical fitting shows threefold symmetry with respect to the azimuthal angle, suggesting the epitaxial arrangement of the monolayer with the Si(111) substrate. The orientation angle of the methyl group estimated from SFG anisotropy was in good agreement with the theoretical prediction.

1. Introduction

Construction of molecular layers on solid surfaces is one of the most important subjects not only for fundamental science but also for a wide range of applications such as wetting control, corrosion inhibition, and molecular- and bioelectronic devices and is one of the key techniques for the development of nanotechnology and nanoscience. A self-assembly (SA) technique in solution has been extensively employed to construct organic layers because a molecularly ordered structure can be prepared very easily without expensive equipment, which is essential for the organic layer formation in ultrahigh vacuum.¹

The most studied SA system is the self-assembled monolayers (SAMs) of alkanethiols on various metals, especially on gold,^{1–3} and SAMs with a wide variety of functionalities have been constructed.^{4,5} The formation process and the structure of the thiol SAMs on gold have been investigated in detail by various techniques including IR spectroscopy,^{6–9} quartz crystal microbalance (QCM),^{10,11} and scanning tunneling microscopy (STM).^{12–15}

It may be more important, however, to construct ordered molecular layers with various functionalities on a semiconductor surface as far as technological applications are concerned. Although several attempts have been made to use GaAs^{16–18} and InP¹⁹ as a substrate, silicon should be the most important semiconductor substrate for organic layer formation at present because of possible applications for molecular and biomolecular devices in conjunction with the advanced silicon technology. There are two major methods to form an organic layer on silicon. One is via the Si–O–Si bond using silane coupling reactions on a preoxidized Si surface. The other is via the direct Si–C bond either on a reconstructed Si(100) surface or on a hydrogen-terminated Si surface using thermal,^{20–23} photochemical,^{24,25} or electrochemical^{26,27} reactions or reactions with radical initiators.^{20,27–29} The latter method is more attractive because

- (1) Ulman, A. *An Introduction to Ultra-Thin Organic Films from Langmuir–Blodgett to Self-Assembly*; Academic Press: San Diego, CA, 1991.
- (2) Finklea, H. O. In *Electrochemistry of Organized Monolayers of Thiols and Related Molecules on Electrodes*; Bard, A. J., Rubinstein, I., Eds.; Marcel Dekker: New York, 1996; Vol. 19, pp 109–335.
- (3) Ulman, A. *Chem. Rev.* **1996**, *96*, 1433–1554.
- (4) Chidsey, C. E. D. *Science* **1991**, *251*, 919–922.
- (5) Uosaki, K.; Kondo, T.; Zhang, X.-Q.; Yanagida, M. *J. Am. Chem. Soc.* **1997**, *119*, 8367–8368.
- (6) Porter, M. D.; Bright, T. B.; Allara, D. L.; Chidsey, C. E. D. *J. Am. Chem. Soc.* **1987**, *109*, 3559–3568.
- (7) Laibinis, P. E.; Whitesides, G. M.; Allara, D. L.; Tao, Y. T.; Parikh, A. N.; Nuzzo, R. G. *J. Am. Chem. Soc.* **1991**, *113*, 7152–7167.
- (8) Sato, Y.; Frey, B. L.; Corn, R. M.; Uosaki, K. *Bull. Chem. Soc. Jpn.* **1994**, *67*, 21–25.
- (9) Ye, S.; Sato, Y.; Uosaki, K. *Langmuir* **1997**, *13*, 3157–3161.
- (10) Shimazu, K.; Yagi, I.; Sato, Y.; Uosaki, K. *Langmuir* **1992**, *8*, 1385–1387.
- (11) Karpovich, D. S.; Blanchard, G. J. *Langmuir* **1994**, *10*, 3315–3322.
- (12) Yamada, R.; Uosaki, K. *Langmuir* **1997**, *13*, 5218–5221.

- (13) Yamada, R.; Uosaki, K. *Langmuir* **1998**, *14*, 855–861.
- (14) Wano, H.; Uosaki, K. *Langmuir* **2001**, *17*, 8224–8228.
- (15) Poirier, G. E. *Chem. Rev.* **1997**, *97*, 1117–1128.
- (16) Baum, T.; Ye, S.; Uosaki, K. *Langmuir* **1999**, *15*, 8577–8579.
- (17) Sheen, C. W.; Shi, J.-X.; Martensson, J.; Parikh, A. N.; Allara, D. J. *Am. Chem. Soc.* **1992**, *114*, 1514–1515.
- (18) Ye, S.; Li, G.; Noda, H.; Uosaki, K.; Osawa, M. *Surf. Sci.* **2003**, *529*, 163–170.
- (19) Gu, Y.; Lin, Z.; Butera, R. A.; Smentkowski, V. S.; Waldeck, D. H. *Langmuir* **1995**, *11*, 1849–1851.
- (20) Linford, M. R.; Fenter, P.; Eisenberger, P. M.; Chidsey, C. E. D. *J. Am. Chem. Soc.* **1995**, *117*, 3145–3155.
- (21) Boukherroub, R.; Morin, S.; Bensebaa, F.; Wayner, D. D. M. *Langmuir* **1999**, *15*, 3831–3835.
- (22) Yu, H.-Z.; Morin, S.; Wayner, D. D. M.; Allongue, P.; de Villeneuve, C. H. *J. Phys. Chem. B* **2000**, *104*, 11157–11161.
- (23) Quayam, M. E.; Kondo, T.; Nihonyanagi, S.; Miyamoto, D.; Uosaki, K. *Chem. Lett.* **2002**, 208–209.
- (24) Terry, J.; Linford, M. R.; Wigren, C.; Cao, R.; Pianetta, P.; Chidsey, C. E. D. *Appl. Phys. Lett.* **1997**, *71*, 1056–1058.
- (25) Effenberger, F.; Gotz, G.; Bidlingmaier, B.; Wezstein, M. *Angew. Chem., Int. Ed.* **1998**, *37*, 2462–2464.
- (26) de Villeneuve, C. H.; Pinson, J.; Bernard, M. C.; Allongue, P. *J. Phys. Chem. B* **1997**, *101*, 2421–2425.
- (27) Fidelis, A.; Ozanam, F.; Chazalviel, J.-N. *Surf. Sci.* **2000**, *444*, L7–L10.
- (28) Bansal, A.; Li, X.; Lauermaier, I.; Lewis, N. S. *J. Am. Chem. Soc.* **1996**, *118*, 7225–7226.

(1) the Si–C bond is expected to be more resistant to hydrolysis than the Si–O–Si bond, (2) a higher structural order is expected because an organic molecule directly bonds to the Si atom of the single crystalline surface, and (3) the thickness control of the oxide is difficult in the former method. Both gas phase^{30,31} and liquid phase^{20–29} reactions have been used to form organic layers via the Si–C bond, but the latter is more useful for practical applications because the former requires expensive UHV equipments to prepare and maintain the reconstructed, clean Si surface.

Not only conformational order but also lateral order and symmetry of a molecular layer are very important in determining the physical and chemical properties of an interface. We have investigated the formation kinetics and development of the molecular order of the octadecyl (C18) monolayer on a hydrogen-terminated Si(111) surface in neat octadecene by attenuated total reflection Fourier transform infrared (ATR FT-IR) and sum frequency generation (SFG) spectroscopy and ellipsometry.²³ Although the conformational order was briefly discussed in a previous article,²³ the lateral order has not been quantitatively investigated thus far. We have briefly reported that the C18 monolayer on a Si(111) surface has an epitaxial arrangement.³² Recently, Ishibashi et al. have shown that the tridecyl (C13) monolayer has an epitaxial arrangement based on azimuthal angle dependent SFG spectra, although a quantitative analysis was not shown.³³

In the present article, we measured the SFG spectra of the C18 monolayer on a hydrogen-terminated Si(111) surface at various azimuthal angles and confirmed that the monolayer is in a nearly *all-trans*, i.e., highly ordered, conformation as well as in threefold lateral symmetry, i.e., epitaxial arrangement of the monolayer with the Si(111) substrate. The SFG spectra were quantitatively analyzed, and lateral alignment with respect to the Si substrate and the tilt angle of the terminal methyl group were estimated.

2. Experimental Section

The hydrogen-terminated Si(111) surface was prepared by chemical etching as previously reported.^{34,35} An *n*-type Si(111) wafer (P-doped, specific resistance: $\sim 3\text{--}5$ Wcm, Shin-Etsu Semiconductors) was first cut and cleaned in a sonication bath of acetone and then with Milli-Q water (resistivity > 18 M Ω cm). The Si wafer was oxidized in hot piranha solution (H₂SO₄/H₂O₂ = 3:1) and etched in a 0.5% HF solution. The Si sample was then reoxidized in a boiling solution of concentrated HCl/H₂O₂/H₂O (1:1:4) for 20 min, etched in a 40% NH₄F solution (Morita Chemical Industries, EL grade) for 5 min, rinsed by Milli-Q water, and finally dried by blowing purified nitrogen gas. The freshly prepared hydrogen-terminated Si(111) substrate was treated in deaerated octadecene (Wako Pure Chemicals) at 200 °C under an Ar (air/water, 99.95%) atmosphere for 2 h. The sample was rinsed with and cooled in deaerated hexadecane (Wako Pure Chemicals) and then further rinsed with deaerated diethyl ether (Wako Pure Chemicals), deaerated ethanol (Wako Pure Chemicals), and deaerated dichloromethane (Wako Pure

Chemicals). After being dried with a stream of Ar, the SFG measurements were carried out. The formation of the monolayer by the present scheme had been previously confirmed by XPS (Rigaku, XPS7000), ATR FT-IR (Biorad, FTS30), and ellipsometry (SOPRA, GES-5) measurements.²³

A detailed description of the SFG system used in the present study has been published elsewhere.^{36,37} Briefly, a Nd:YAG laser (PL2143B, EKSPILA) with 25 ps pulse width and repetition rate of 10 Hz was employed to pump an OPG/OPA/DFG system, which generates tunable infrared radiation. The second harmonic output (532 nm) from the Nd:YAG laser was used as the visible light. Loosely focused visible and infrared beams of 0.05 mJ/pulse and 0.2 mJ/pulse, respectively, were overlapped at the surface of the Si substrate, which was placed on a rotation stage. The visible and infrared lights were in the same plane of incidence, and the angle of incidence of the visible (θ_{vis}) and infrared (θ_{IR}) lights were about 70° and 50°, respectively. The SFG, visible, and IR lights were *p*-, *p*-, and *p*- polarized, respectively (abbreviated as *ppp*).³⁸ An azimuthal angle was defined to be the angle between the $[2\bar{1}\bar{1}]$ direction of the Si(111) substrate and the plane of incidence. The SFG signal was separated from the reflected visible and IR lights by passing through irises and a monochromator (Oriel Instruments, MS257) and was detected by a photomultiplier tube (PMT: Hamamatsu, R3896) and was normalized to the intensities of the infrared and visible beams. The SFG measurements were carried out in air at room temperature (ca. 22 °C).

3. Theoretical Basis

A number of reviews have been published about the theoretical background of SFG and its applications.^{39–41} SFG is one of the second-order nonlinear optical processes in which two photons at frequencies of ω_1 and ω_2 generate one photon of sum frequency at $\omega_3 = \omega_1 + \omega_2$. The second-order nonlinear optical processes including SFG do not take place in media with inversion symmetry under the electric dipole approximation but are active at the interface between these media where the inversion symmetry is necessarily broken. In the IR-visible SFG measurement, a visible laser beam (ω_{vis}) and a tunable infrared laser beam (ω_{IR}) are overlapped at an interface, and the SFG signal (ω_{SFG}) is measured by scanning ω_{IR} while keeping ω_{vis} constant.

We define the axis systems as depicted in Figure 1. In the laboratory-fixed axis system ($I, J, K = X, Y, Z$), the Z -axis is surface normal and the X – Z plane is the incident plane of the visible and infrared beams. In the surface-fixed axis system ($i, j, k = x, y, z$), the x -axis is set in the $[2\bar{1}\bar{1}]$ direction of the Si(111) surface and the z -axis coincides with the Z -axis. The angle between the X – Z and the x – z planes is represented by γ . In the molecular-fixed axis system ($p, q, r = \xi, \eta, \zeta$), the ζ -axis is taken to coincide with C_3 symmetry axis of a methyl (CH₃) group and the ξ – η plane is one of the C–C–H planes of the CH₃ group. The θ , ψ , and ϕ are defined as angles between the z - and ζ -axes, the projection of the ζ -axis on the surface and the x -axis, and y' - and η -axes, respectively, where y' -axis is the y -axis rotated by ψ (see Figure 1).

(29) Bansal, A.; Lewis, N. S. *J. Phys. Chem. B* **1998**, *102*, 1067–1070.

(30) Bozack, M. J.; Taylor, P. A.; Choyke, W. J.; Yates, J. T., Jr. *Surf. Sci.* **1986**, *177*, L933–L937.

(31) Lopinski, G. P.; Wayner, D. D. M.; Wolkow, R. A. *Nature* **2000**, *406*, 48–51.

(32) Miyamoto, D.; Nihonyanagi, S.; Kondo, T.; Uosaki, K. *Abstracts*, 81st Spring Meeting of the Chemical Society of Japan, Tokyo, March 26–29, 2002; The Chemical Society of Japan: Tokyo; 3 D2-36.

(33) Ishibashi, T.; Ara, M.; Tada, H.; Onishi, H. *Chem. Phys. Lett.* **2003**, *367*, 376–381.

(34) Higashi, G. S.; Chabal, Y. J.; Trucks, G. W.; Raghavachari, K. *Appl. Phys. Lett.* **1990**, *56*, 656–658.

(35) Ye, S.; Ichihiro, T.; Uosaki, K. *Appl. Phys. Lett.* **1999**, *75*, 1562–1564.

(36) Ye, S.; Saito, T.; Nihonyanagi, S.; Uosaki, K.; Miranda, P. B.; Kim, D.; Shen, Y. R. *Surf. Sci.* **2001**, *476*, 121–128.

(37) Ye, S.; Nihonyanagi, S.; Uosaki, K. *Phys. Chem. Chem. Phys.* **2001**, *3*, 3463–3469.

(38) SFG measurements with other polarization combinations such as *ssp* were attempted so that more detailed analyses were possible, but we were not able to obtain these spectra due to various experimental restrictions, mostly due to the lower values of the product of Fresnel factors with the polarization combination other than *ppp*.

(39) Shen, Y. R. *Proc. Natl. Acad. Sci. U.S.A.* **1996**, *93*, 12104–12111.

(40) Bain, C. D. *J. Chem. Soc., Faraday Trans.* **1995**, *91*, 1281–1296.

(41) Miranda, P. B.; Shen, Y. R. *J. Phys. Chem. B* **1999**, *103*, 3292–3307.

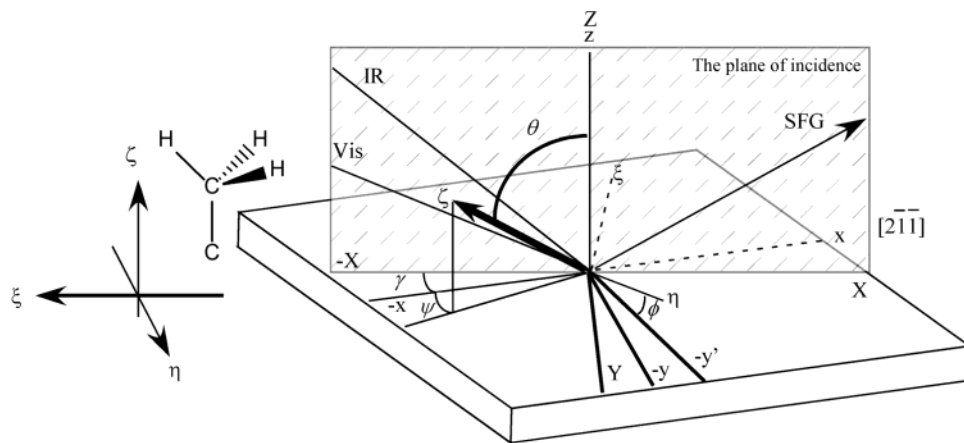


Figure 1. Schematic drawing of the definitions of the laboratory-, surface- and molecular-fixed axis systems. The γ was defined as the angle between the $[2\bar{1}1]$ direction of the Si(111) substrate and the plane of incidence.

The SFG intensity (I_{SFG}) generated by the input visible and infrared fields with intensities I_{Vis} and I_{IR} , respectively, can be expressed by the following equations:^{40,42}

$$I_{\text{SFG}} = \frac{8\pi^3 \omega_{\text{SFG}}^2 \sec^2 \theta_{\text{SFG}}}{c^3} |\vec{\chi}_{\text{eff}}^{(2)}|^2 I_{\text{Vis}} I_{\text{IR}} \quad (1a)$$

$$\vec{\chi}_{\text{eff}}^{(2)} = |\chi_{\text{NR}}^{(2)}| e^{i\epsilon} + \sum \frac{\vec{A}_{\text{eff},n}}{\omega_{\text{IR}} - \omega_n + i\Gamma_n} \quad (1b)$$

where $\vec{\chi}_{\text{eff}}^{(2)}$ is an effective second-order susceptibility, θ_{SFG} is the angle of the sum frequency output with respect to the surface normal, and c is the speed of light in a vacuum. $\chi_{\text{NR}}^{(2)}$, ϵ , $\vec{A}_{\text{eff},n}$, and Γ_n are the second-order susceptibility corresponding to the nonresonant component, the relative phase between the resonant and nonresonant contributions, the effective amplitude, and the damping constant of a surface vibration or rotation mode with frequency ω_n , respectively.

A resonant molecular hyperpolarizability near the n th vibrational state in the molecular fixed coordinates ($\beta_{pqr,n}$) is expressed as

$$\beta_{pqr,n} = \frac{a_{pqr,n}}{\omega_{\text{IR}} - \omega_n + i\Gamma_n} \quad (2)$$

where $a_{pqr,n}$ is the product of a Raman polarization tensor ($\alpha_{pq,n}$) and vibrational transition dipole moment ($\mu_{r,n}$), with $\langle g|$ being ground state and $\langle v|$ being n th vibrational state:⁴³

$$a_{pqr,n} = \langle g | \alpha_{pq} | v \rangle \langle v | \mu_r | g \rangle \quad (3)$$

Here, the relation between $\vec{A}_{\text{eff},n}$ and $a_{pqr,n}$ is given by:

$$\vec{A}_{\text{eff},n} = N \sum_{I,J,K} F_{IJK} \langle a_{IJK,n} \rangle = N \sum_{I,J,K} F_{IJK} \langle u_{IJK,pqr} a_{pqr,n} \rangle \quad (4)$$

where N and $u_{IJK,pqr}$ represent the total number of the surface molecules and a transformation coefficient, explicit expression of which is presented in ref 44. The brackets $\langle \rangle$ denote the

(42) Shen, Y. R. In *Sum Frequency Generation (SFG) Spectroscopy*; Field, R. W., Hirota, E., Maier, J. P., Tsuchiya, S., Eds.; Blackwell Science Ltd.: Oxford, 1998; pp 249–270.

(43) Hirose, C.; Yamamoto, H.; Akamatsu, N.; Domen, K. *J. Phys. Chem.* **1993**, *97*, 10064–10069.

(44) Hirose, C.; Akamatsu, N.; Domen, K. *Appl. Spectrosc.* **1992**, *46*, 1051–1072.

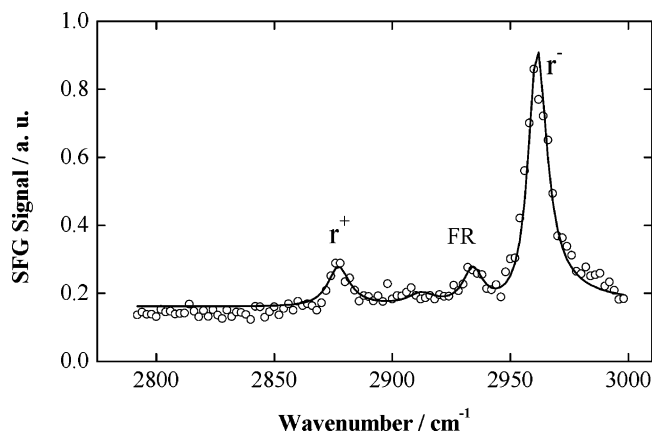


Figure 2. SFG spectrum of the Si(111)–C18 monolayer at the azimuthal angle $\gamma = 0$ in the CH stretching frequency region with the fitted curve using eq 1.

ensemble average. F_{IJK} is a combination of Fresnel factors and is represented as:^{42,45}

$$F_{IJK} = \hat{e}_I(\omega_{\text{SFG}}) L_I(\omega_{\text{SFG}}) \times \hat{e}_J(\omega_{\text{Vis}}) L_J(\omega_{\text{Vis}}) \times \hat{e}_K(\omega_{\text{IR}}) L_K(\omega_{\text{IR}}) \quad (5)$$

where $L_I(\omega_{\text{SFG}})$, $L_J(\omega_{\text{Vis}})$, and $L_K(\omega_{\text{IR}})$ are the Fresnel factors for the SFG, visible, and IR beams, respectively, and $\hat{e}_I(\omega_{\text{SFG}})$, $\hat{e}_J(\omega_{\text{Vis}})$, and $\hat{e}_K(\omega_{\text{IR}})$ are the unit polarization vectors for the SFG, visible, and IR beams, respectively. For the ppp polarization combination, $\vec{A}_{\text{eff},n}$ is given by:

$$\vec{A}_{\text{eff},n} = N \{ F_{ZZZ} \langle a_{ZZZ} \rangle - F_{XXZ} \langle a_{XXZ} \rangle - F_{XZZ} \langle a_{XZZ} \rangle + F_{ZXX} \langle a_{ZXX} \rangle + F_{ZXX} \langle a_{ZXX} \rangle - F_{ZXX} \langle a_{ZXX} \rangle + F_{ZXX} \langle a_{ZXX} \rangle - F_{XXX} \langle a_{XXX} \rangle \} \quad (6)$$

4. Results and Discussion

1. Conformation. Figure 2 shows an SFG spectrum in the CH stretching frequency region of a Si(111)–C18 monolayer at $\gamma = 0$. The open circles and solid line represent the experimentally observed SFG signals and a fitted curve using eq 1, respectively. The spectrum very much resembles the previously reported SFG spectra of the octadecyltrichlorosilane (OTS) monolayer on a fused quartz substrate with ppp polariza-

(45) Kim, D.; Oh-e, M.; Shen, Y. R. *Macromolecules* **2001**, *34*, 9125–9129.

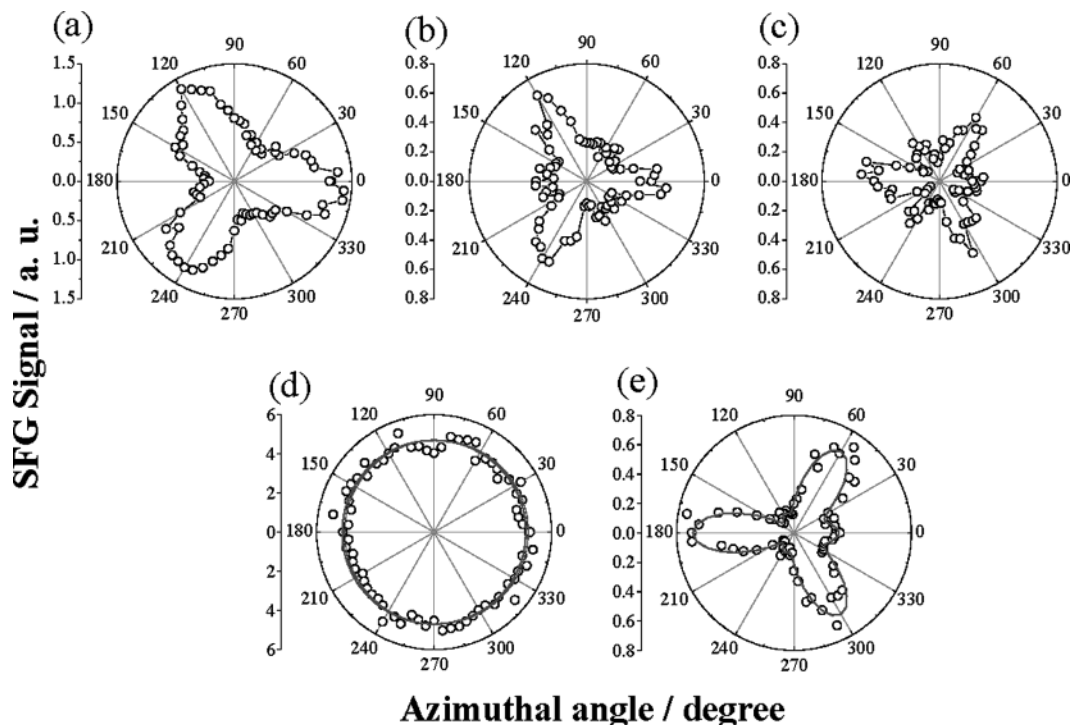


Figure 3. Rotation anisotropy of the SFG intensity of the Si(111)–C18 monolayer at (a) 2962 cm^{-1} , (b) 2878 cm^{-1} , and (c) 2800 cm^{-1} and of Si(111)–H at (d) 2083 cm^{-1} and (e) 2120 cm^{-1} as a function of the azimuthal angle.

tion.⁴⁶ The three peaks observed at 2878, 2945, and 2962 cm^{-1} can be assigned to the CH symmetric vibration (r^+), Fermi resonance between r^+ and the CH bending overtone, and the CH asymmetric vibration (r^-), respectively, of the terminal methyl (CH_3) group. Two peaks due to the CH symmetric stretching (d^+) at 2850 cm^{-1} and asymmetric stretching (d^-) at 2917 cm^{-1} of the methylene (CH_2) group are very weak compared to those of the CH_3 group. These results indicate that the octadecyl chain in the monolayer is essentially in an *all-trans* conformation. In this conformation, only the terminal CH_3 group, which is in noncentrosymmetry, contributes to the SFG spectrum because CH_2 groups are approximately in inversion symmetry and are, therefore, almost SFG inactive. Thus, the formation of a highly organized octadecyl monolayer with a very low gauche density on the Si(111) surface²³ is confirmed.⁴⁷

Recently, Ishibashi et al. reported the presence of small peaks due to the methylene modes in the SFG spectra of alkyl monolayers of various chain lengths using an SFG system with a *fs* laser.³³ They suggested that the peaks were due to the methylene modes originated from the twisted parts of alkyl chain ($\text{Si}-\text{C}-\text{C}-$). The present result based on the SFG system with the *ps* laser does not show the methylene modes. There are several possibilities to account for this discrepancy. The sample preparation methods are slightly different, and the time domain of the SFG measurements are also different. To clarify the cause of the discrepancy between the present results and Ishibashi's, SFG measurements using both *ps* and *fs* SFG spectrometers for exactly the same sample are now under way.

2. Rotation Anisotropy. One of the advantages of SFG spectroscopy compared to infrared absorption spectroscopy

(IRAS) is the ability to determine the lateral symmetry based on the azimuthal angle dependence of the SFG spectra, i.e., rotation anisotropy of the SFG spectra. Figure 3 shows the azimuthal angle dependencies of the SFG intensity, i.e., rotation anisotropy, at (a) 2962 cm^{-1} for r^- , (b) 2878 cm^{-1} for r^+ , and (c) 2800 cm^{-1} where no peak was observed. Threefold patterns were observed for the peaks at 2962 and 2878 cm^{-1} , suggesting the existence of lateral symmetry in the monolayer assembly. A threefold pattern was also observed at 2800 cm^{-1} where no peak corresponding to the monolayer exists and only the nonresonant component contributes to the SFG spectrum. It must be noted, however, the threefold pattern at 2800 cm^{-1} is different from those at 2962 and 2878 cm^{-1} by 60°. At least two possible causes for the SFG rotation anisotropy have been proposed. Yeganeh et al. reported the threefold pattern in the SFG signal at the alkyl-thiol SAM on a gold (111) surface and attributed the anisotropy to the anisotropy of bonding sites.⁴⁸ Hirose et al. observed anisotropy for the SFG signal of the methyl stretching mode of multilayered LB films of cadmium arachidate and suggested the anisotropy to be due to the anisotropy of the molecular orientation of alkyl chains, which arose from withdrawing process in the LB multilayer formation.⁴³ Shen et al. and Miyamae et al. also reported the anisotropy of SFG intensities of polymer films and assigned it to be due to the anisotropy of the molecular orientation of polymer chains, which arose from the rubbing or machine drawing process.^{45,49,50} For the present results, because the SFG intensity of a hydrogen-terminated Si(111) at 2083 cm^{-1} corresponding to the Si–H vibration, whose symmetry axis is perpendicular to the surface, is essentially independent of the azimuthal angle (Figure 3d)

(46) Shen, Y. R. *Nature* **1989**, *337*, 519–525.

(47) If SFG spectra were available with other polarization combinations, the analyses would be simpler and more accurate, but only the SFG spectra with ppp polarization were obtained.³⁸

(48) Yeganeh, M. S.; Dougal, S. M.; Polizzotti, R. S.; Rabinowitz, P. *Phys. Rev. Lett.* **1995**, *74*, 1811–1814.

(49) Wei, X.; Zhuang, X.; Hong, S. C.; Goto, T.; Shen, Y. R. *Phys. Rev. Lett.* **1999**, *82*, 4256–4259.

(50) Miyamae, T.; Nozoe, H. *J. Photochem. Photobiol., A* **2001**, *145*, 93–99.

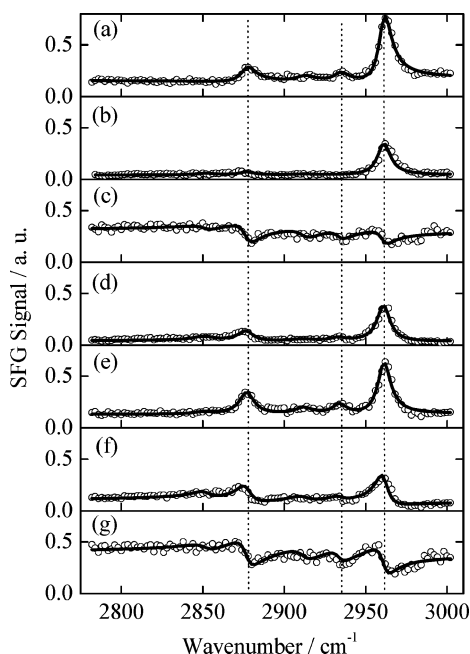


Figure 4. The SFG spectra of a Si(111)-C18 monolayer obtained at various azimuthal angles (○) with the fitted curves to eq 1 (solid line). (a) 0, (b) 30, (c) 60, (d) 90, (e) 120, (f) 150, and (g) 180°.

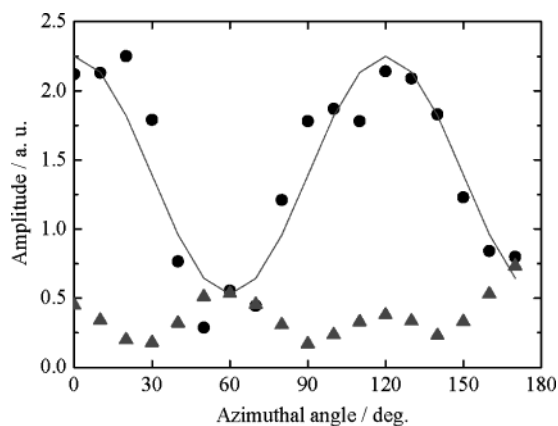


Figure 5. Plots of \bar{A}_{eff,r^-} (●) and $\chi_{\text{NR}}^{(2)}$ (▲) determined by the fitting of the SFG spectra shown in Figure 4 against the azimuthal angle. The solid line shows the fitted curve to eq 12.

despite the fact that the SFG signal at 2120 cm^{-1} corresponding to the nonresonant response from the silicon substrate produces a threefold symmetry pattern (Figure 3e), it is reasonable to conclude that the observed SFG anisotropy originated not from the anisotropy of the binding site but from the anisotropy of the orientation of the tilted alkyl chains.

To quantitatively discuss the symmetry of the methyl group, it is essential to study the azimuthal angle dependence of the effective amplitude of the CH signal. Figure 4 shows the SFG spectra at various azimuthal angles with the fitted curves (solid line) to eq 1. It is clear that the shape and position of the resonant peaks as well as the nonresonant background level strongly depended on the azimuthal angle. Thus, the nonresonant contribution should be separated from the SFG spectra using eq 1. The amplitudes of the r^- mode ($\bar{A}_{\text{eff},n}$) and nonresonant contribution ($\chi_{\text{NR}}^{(2)}$) were determined by fitting to eq 1 and are plotted against the azimuthal angle as shown in Figure 5. A threefold symmetry of the r^- mode is clearly demonstrated.

$\chi_{\text{NR}}^{(2)}$ also shows threefold symmetry, but the phase angle is different from that of the r^- mode.

If we assume C_{3v} symmetry for the methyl group, the nonvanishing components of the amplitude of the molecular hyperpolarizability, $a_{pqr,n}$, for the r^- mode of the methyl group are:⁴³

$$a_{\xi\xi\xi} = a_{\eta\xi\eta}, a_{\zeta\xi\xi} = a_{\zeta\eta\eta} \quad (7)$$

$$a_{\xi\xi\xi} = -a_{\eta\eta\xi} = -a_{\xi\eta\eta} = -a_{\eta\xi\eta} \quad (8)$$

where the subscript r^- is dropped for simplicity. Since the experiments were carried out at room temperature, the torsional angle of the methyl group is expected to be randomly distributed,⁴³ and the components in eq 8 disappear in the ensemble average defined in eq 4.⁴⁴ Moreover, since the Raman tensor components $\alpha_{\xi\xi}$ and $\alpha_{\xi\xi}$ are equal,⁵¹ $a_{\xi\xi\xi}$ and $a_{\xi\xi\xi}$ should be also equal according to eq 3.⁵² The nonvanishing a_{pqr} components for the r^- mode are then:

$$a_{\xi\xi\xi} = a_{\eta\xi\eta} = a_{\zeta\xi\xi} = a_{\zeta\eta\eta} \quad (9)$$

If the orientation of the tilted alkyl chain has C_{3v} symmetry, the nonvanishing components in the laboratory-fixed axis system, a_{IJK} , related to the r^- mode can be written as follows with the assumption of random distribution of the torsional angle of the methyl group.⁴⁴

$$a_{ZZZ} = 2a_{\zeta\xi\xi}(\cos\theta - \cos^3\theta), a_{XXX} = -a_{\zeta\xi\xi}(\cos\theta - \cos^3\theta)$$

$$a_{ZXX} = a_{XZX} = a_{\zeta\xi\xi} \cos^3\theta, a_{XXX} = -\frac{a_{\zeta\xi\xi}}{2} \sin^3\theta \times \cos[3(\gamma + \psi)] \quad (10)$$

Since θ_{SFG} and θ_{vis} are almost equal and the refractive indices of silicon at the SFG and visible wavelengths are not much different, the Fresnel factors F_{ZZX} and F_{XZX} are approximately the same and, therefore, the third and the fourth terms in eq 6 are canceled out. Equation 6 can then be rewritten as:

$$A_{\text{eff},r^-} = 2a_{\zeta\xi\xi}(\langle\cos\theta\rangle - \langle\cos^3\theta\rangle)NF_{ZZZ} + a_{\zeta\xi\xi}(\langle\cos\theta\rangle - \langle\cos^3\theta\rangle)NF_{XZX} + \frac{a_{\zeta\xi\xi}}{2}NF_{XXX}(\sin^3\theta)\langle\cos[3(\gamma + \psi)]\rangle \quad (11)$$

If we assume a delta function for the distribution of ψ , i.e., the distribution being negligible, and introduce parameters U for the first and second (isotropic) terms and V for $(a_{\zeta\xi\xi}/2)NF_{XXX} \sin^3\theta$ (anisotropic) in the third term in eq 11, eq 11 can be written as:

$$\bar{A}_{\text{eff},n} = U + V \cos[3(\gamma + \psi)] \quad (12)$$

The experimental results were well reproduced by eq 12 with the angle offset $\psi = 0$. Thus, we can conclude that the terminal methyl groups in the octadecyl monolayer aligned in the particular directions of $\psi = 0^\circ$, 120° , and 240° with respect to the in-plane orientation, resulting in C_{3v} symmetry. A possible lateral arrangement that has C_{3v} symmetry is illustrated in Figure 6. In the present model, the octadecyl chains tilt toward either $[\bar{2}11]$, $[\bar{1}21]$, or $[11\bar{2}]$ direction in each domain, forming C_{3v} symmetry as a result.

3. Tilt Angle of the Methyl Group. In most cases, the tilt angles of the terminal methyl groups of the alkyl monolayer

(51) Hirose, C.; Akamatsu, N.; Domen, K. *J. Chem. Phys.* **1992**, *96*, 997–1004.
(52) Watanabe, N.; Yamamoto, H.; Wada, A.; Domen, K.; Hirose, C. *Spectrochim. Acta* **1994**, *50A*, 1529–1537.

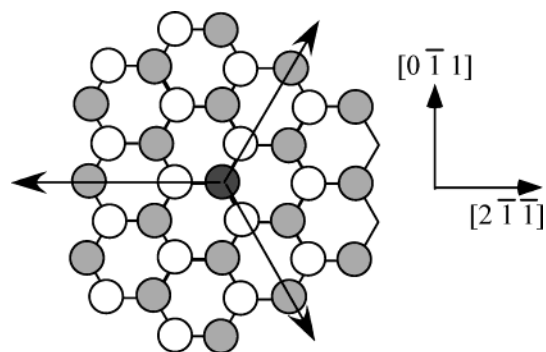


Figure 6. Schematic model of the lateral arrangement of the alkyl chain with gray and white balls denoting the silicon atoms at the top and at the second layer, respectively. Arrows denote the dipole moment of the methyl group.

on a metal and quartz and of the polymer side chain have been estimated by many researchers by comparing the SFG intensities of the r^+ mode with the ssp and sps polarization combinations or those of the r^+ and r^- modes with the ssp polarization combination.^{43,53,54} The calculation of tilt angle of the methyl group can also be carried out by comparing the value of the anisotropic term to the isotropic term in eq 12. This calculation has an advantage because the value of the ratio of the susceptibility tensors ($a_{\xi\xi\xi,r^-}/a_{\xi\xi\xi,r^+}$, $a_{\xi\xi\xi,r^+}/a_{\xi\xi\xi,r^-}$), which is necessary to compare the SFG intensities for the r^+ and r^- modes,^{43,53,55,56} is not required.

By combining eqs 11 and 12, the ratio between U and V is given as

$$\frac{U}{V} = \frac{2(\langle \cos \theta \rangle - \langle \cos^3 \theta \rangle)(2F_{zzz} + F_{xxx})}{F_{xxx} \langle \sin^3 \theta \rangle} \quad (13)$$

The ensemble average of the tilt angle of the terminal methyl group is expressed as follows by assuming a Gaussian distribution:⁴³

$$\begin{aligned} \langle \cos^m \theta \rangle &= \int_{-1}^1 \cos^m \theta \cdot f(\cos \theta) d(\cos \theta) \\ \langle \sin^m \theta \rangle &= \int_{-1}^1 \sin^m \theta \cdot f(\sin \theta) d(\sin \theta) \\ f(\theta) &= C \exp \left[-\frac{(\theta - \theta_0)^2}{2\sigma^2} \right] \end{aligned} \quad (14)$$

where C , θ_0 , and σ are the normalization constant, the center angle, and the root-mean square width of the distribution, respectively. The validity of the Gaussian distribution has been discussed by Wang et al.⁵⁷ Fresnel factors F_{ZZZ} , F_{XXZ} , and F_{XXX} are estimated to be 0.17, 0.041, and 0.031, respectively, using refractive indices of silicon that are $n(\omega_{\text{SFG}}) = 4.55 + 0.134i$,

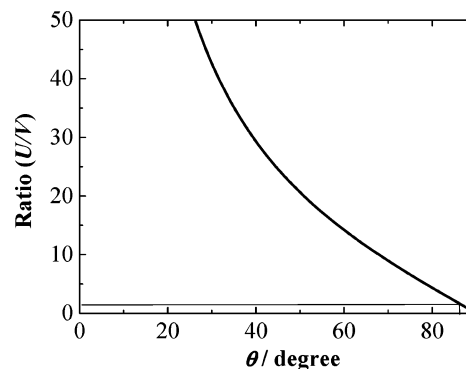


Figure 7. Plot of the ratio (U/V) versus the tilt angle of the methyl group (θ). The bars show the experimental value obtained from Figure 5.

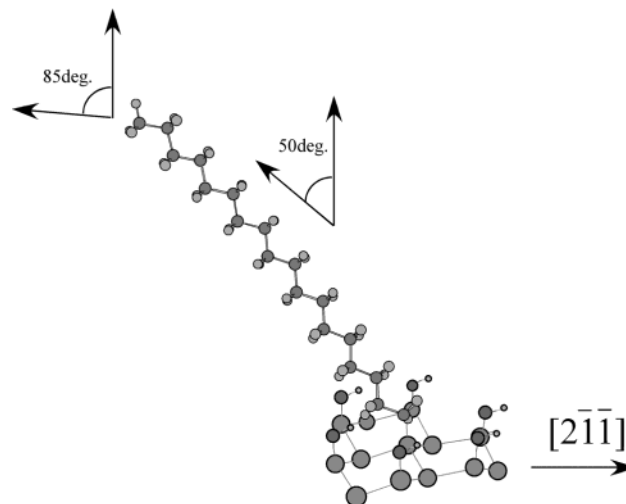


Figure 8. Model of the possible orientation of the octadecyl chain. The alkyl chain is essentially in the all-trans conformation and epitaxially arranged, being tilted toward the $\{211\}$ direction. The tilt angle of the methyl group is estimated to be about 85° with respect to the surface normal.

$n(\omega_{\text{vis}}) = 4.14 + 0.045i$, $n(\omega_{\text{IR}}) = 3.42 + 2.0 \times 10^{-7}i$,⁵⁸ with the assumption that the refractive index of the interface is of the monolayer, i.e., $n' = 1.42$.⁵⁹ The ratio U/V is then plotted against the tilt angle of the methyl group (θ) as shown in Figure 7. Since the experimentally determined value of U/V is ~ 2 , the angle θ is determined to be about 85° , assuming $\sigma = 0$, i.e., the distribution is neglected. Even in the case of $\sigma = 10$ and $\sigma = 20$, θ is still about 85° . The corresponding tilt angle of the alkyl chain is ca. 50° , which is in qualitative agreement with the previously reported value of ca. 45° estimated from the IR and X-ray reflectivity²⁰ as well as the theoretical calculations.^{60,61}

5. Conclusion

The structure of an octadecyl monolayer formed on a hydrogen-terminated Si(111) surface was studied by infrared-visible SFG spectroscopy. It was confirmed that the monolayer

(53) Bell, G. R.; Bain, C. D.; Ward, R. N. *J. Chem. Soc., Faraday Trans.* **1996**, *92*, 515–523.

(54) Wang, J.; Chen, C.; Buck, S. M.; Chen, Z. *J. Phys. Chem. B* **2001**, *105*, 12118–12125.

(55) Gautam, K. S.; Schwab, A. D.; Dhinojwala, A.; Zhang, D.; Dougal, S. M.; Yeganeh, M. S. *Phys. Rev. Lett.* **2000**, *85*, 3854–3857.

(56) The tilt angle of the terminal methyl groups of the alkyl monolayer was estimated by comparing the SFG intensities of r^+ and r^- modes at $\gamma = 0$, assuming values of susceptibility tensor ratios $a_{\xi\xi\xi,r^-}/a_{\xi\xi\xi,r^+} = 4.21$ and $a_{\xi\xi\xi,r^+}/a_{\xi\xi\xi,r^-} = 4.00$.^{42,50} However, the estimated value of $A_{r^+}(\gamma = 0)/A_{r^-}(\gamma = 0)$ was too large to be a possible value for any tilt angle of a methyl group. The ratio $a_{\xi\xi\xi,r^-}/a_{\xi\xi\xi,r^+}$ seems to be smaller than 4.21, which we assumed.

(57) Wang, J.; Paszti, Z.; Even, M. A.; Chen, Z. *J. Am. Chem. Soc.* **2002**, *124*, 7016–7023.

(58) Palik, E. D. *Handbook of Optical Constants of Solids*; Academic Press: Orlando, FL, 1985.

(59) Although the value of $n' = 1.42$, which is a value of liquid dodecane, was used for the calculation, there is some controversy about the value of n' for the monolayer. Our recent spectroellipsometry measurement showed the refractive index of C18 monolayer on silicon in air was nearly 1.5. The calculated tilt angle of methyl group is, however, affected only slightly by the value of n' . It is 88, 85, and 83° for $n' = 1.2$, 1.42, and 1.5, respectively.

(60) Sieval, A. B.; van den Hout, B.; Zuilhof, H.; Sudholter, E. J. R. *Langmuir* **2001**, *17*, 2172–2181.

(61) Zhang, L.; Wesley, K.; Jiang, S. *Langmuir* **2001**, *17*, 6275–6281.

was essentially in the *all-trans*, i.e., highly ordered, conformation by SFG spectra in the CH vibration region. It was found that the monolayer was epitaxially arranged with the Si(111) substrate with C_{3v} anisotropy and the alkyl chains tilt toward the $\{\bar{2}11\}$ directions. The tilt angle of the methyl group was estimated to be about 85° , which corresponds to ca. 50° of the tilt angle of the alkyl chain. The possible orientation model is depicted in Figure 8.

Acknowledgment. This work was partially supported by Grants-in-Aid for Scientific Research from the Ministry of

Education, Culture, Sports, Science and Technology, Japan (No. 13304047). S.N. acknowledges the Japan Society for Promotion of Science (JSPS) for a fellowship. Mr. Kitazawa of Shin-Etsu Semiconductor is acknowledged for the donation of the Si(111) wafers. Professor Kondo is acknowledged for his help with the sample preparation and useful comments. Professor Shimazu is acknowledged for his help with the XPS measurements. We are grateful to Professor Yagi for his useful comments.

JA049911P